Green Chemistry

PAPER

View Article Online
View Journal | View Issue

Cite this: *Green Chem.*, 2025, **27**, 14131

Efficient hydrothermal pretreatment of mixed PHA/PLA and subsequent continuous anaerobic fermentation into VFA

Yong Jin, Ralf Beckmans, Kasper D. de Leeuw and David P. B. T. B. Strik *

Recycling biobased biodegradable plastics such as polyhydroxyalkanoates (PHA) and polylactic acid (PLA) is promising for developing a circular economy. This study presents the development of a combined technology to convert PHA and PLA into C_2–C_6 monocarboxylates *via* batch hydrothermal pretreatment (HTP, 150 °C) and continuous open-culture fermentation. HTP experiments revealed that supplementing PHA with carboxylic acids or PLA strongly enhanced depolymerization, reaching up to 91 ± 4% dissolution compared to 46 ± 8% without supplements. In sequential fermentation, acetate and *n*-butyrate were the dominant products. Co-fermentation of PHA hydrolysates (~10 g L^{-1} 3-hydroxybutyrate) and PLA hydrolysates (5 g L^{-1} lactate) yielded acetate (4.4 g L^{-1}), *n*-butyrate (8.0 g L^{-1}), and *n*-caproate (0.3 g L^{-1}), while reducing alkali demand for pH control relative to PHA-only hydrolysates. Overall, ~90% of the bioplastics' chemical oxygen demand (COD) was recovered as carboxylates, with a *n*-butyrate COD selectivity of 71%. Ethanol supplementation (7 g L^{-1}) further increased *n*-butyrate production to 10.1 g L^{-1}, although ethanol was not fully consumed. Microbial bacteria community analysis identified *Clostridium tyrobutyricum* as the dominant species, likely driving *n*-butyrate production and capable of utilizing crotonate, 3-hydroxybutyrate, and lactate. This study demonstrates, for the first time, the feasibility of continuous open-culture fermentation for valorizing mixed bioplastic hydrolysates into carboxylates.

Received 30th May 2025,
Accepted 7th October 2025

DOI: 10.1039/d5gc02732b

rsc.li/greenchem

Green foundation

1. Recycling bioplastics through a carboxylate platform can help close the carbon loop, but effective pretreatment is essential. This study introduces a potential scalable hydrothermal pretreatment strategy that achieves up to 91% PHA and 97% PLA dissolution without chemical catalysts supply, enabling high-yield production of fermentation-ready hydrolysates from commercial plastic products.
2. For the first time, continuous open-culture fermentation of PHA and PLA hydrolysates achieved ~90% COD conversion efficiency and 71% *n*-butyrate selectivity. This demonstrates that complex biodegradable plastic mixtures can be valorized into valuable C_2–C_6 monocarboxylates.
3. *Clostridium tyrobutyricum* likely emerged as a key functional species capable of converting 3-hydroxybutyrate, crotonate, and lactate into carboxylates. The bioreactor microbiome enrichment, along with pH self-regulation from lactate metabolism, significantly improved process performance and reduced external base demand, showing promise for industrial bioplastic recycling.

Introduction

Polyhydroxyalkanoates (PHA) and polylactic acid (PLA) are biobased biodegradable plastics that have emerged as promising alternatives to conventional petrochemical plastics, such as polypropylene (PP) and polyethylene (PE).[1] PHA encompasses a range of polymers composed of different monomers, such as polyhydroxybutyrate (PHB) and poly(3-hydroxybutyrate-*co*-3-hydroxyvalerate) (PHBV).[2] PLA is a thermoplastic aliphatic polyester derived from lactic acid.[3] PHA and PLA accounted for approximately 4% and 37% of the 2024 global bioplastics production capacities, respectively. The annual growth is projected at 57% for PHA and 21% for PLA until 2029.[4] These materials are increasingly used in packaging, agricultural mulch films and textiles.[5–7]

Despite their biodegradability, the end-of-life management of PHA and PLA remains problematic. The mechanical and degradation properties of biodegradable plastic products vary depending on their composition, such as the PHA-to-PLA ratio and the presence of plasticizers.[8] Biodegradation is typically facilitated by controlled environmental conditions, including microbial activity, elevated temperatures, and sufficient humidity.[9] Current disposal methods such as composting, anaerobic digestion, and in-field degradation often result in

Environmental Technology, Wageningen University & Research, Axis-Z, Bornse Weilanden 9, 6708 WG Wageningen, the Netherlands. E-mail: david.strik@wur.nl

incomplete conversion and limited energy or carbon recovery.[10,11] Other approaches, including incineration and landfilling, increase CO_2 emissions and environmental burdens.[12] Moreover, both natural and engineered biodegradation processes (including the anaerobic digestion and combustion of biogas) contribute significantly to greenhouse gas emissions, undermining the environmental promise of bioplastics.[13]

To address these limitations, recent studies have proposed the valorization of biodegradable plastics *via* anaerobic fermentation of hydrolysates into carboxylates which have broad industrial applications.[3,14,15] For example, these carboxylates serve as precursors for feed additives, lubricants, pharmaceuticals, cosmetics, and bioplastics.[16–18] This way biodegradable plastic recycling can become part of the "carboxylate platform" or volatile fatty acid platform enabling carbon recovery and possibly lead to less CO_2 emissions compared to composting. Companies such as ChainCraft, Afyren, BioVeritas, and Capro-X are already developing commercial carboxylate production processes from organic waste streams.[19–22] A wide range of model compounds of biodegradable plastics, like crotonate, lactate, and ethanol, have already been shown to yield acetate, *n*-butyrate, and *n*-caproate under open-culture fermentation.[3,14,23–26]

However, direct anaerobic fermentation of raw PHA and PLA remains inefficient. Without pretreatment, PHA shows low conversion efficiencies (10–18%), and PLA is largely recalcitrant under mesophilic conditions.[27] To enhance biodegradability, various pretreatment methods have been explored, including enzymatic, chemical, pyrolytic, and hydrothermal processes.[28] Enzymatic hydrolysis is effective but still limited by the availability of functional enzymes capable of degrading the broad type of biodegradable plastics.[29] Hydrothermal pretreatment (HTP) at ≥200 °C has proven effective for depolymerizing PHA into 3-hydroxybutyric acid and crotonic acid.[30,31] PLA was effectively converted into lactic acid at 70 °C.[3] Depending on temperature and co-solutes, HTP can yield reactive intermediates such as oligomers and carboxylic acids that promote further depolymerization. For example, 3-hydroxybutyric acid and crotonic acid have been found to enhance PHA hydrolysis at 200 °C, while PLA-derived oligomers have been shown to promote PHA degradation even at 37 °C.[30,32] Given these findings, it is hypothesized that increased PLA dissolution during hydrolysis of a PHA/PLA mixture at hydrothermal process (>100 °C) may lead to accelerated depolymerization of PHA.

Although pure culture studies have elucidated microbial pathways for fermenting 3-hydroxybutyrate (3-HB) and crotonate into carboxylates,[33–36] there is limited understanding of microbial community dynamics during anaerobic conversion of bioplastics. Previous research has shown that mixed cultures, including non-pretreated anaerobic sludge and rumen-based consortia, can ferment PHA and PLA hydrolysates into carboxylates.[14,27] However, the microbial communities involved as well as the methanogens suppression mechanisms were not studied. Since methanogens compete with fermentative bacteria, their inhibition—using either chemical additives such as 2-bromoethanesulfonate sodium (BES) or process parameters like pH, organic loading rate (OLR), hydraulic retention time (HRT), and inoculum heat pretreatment—is critical for selective carboxylate production.[23,37,38] Moreover, it is also shown that BES can affect the carboxylate fermentation process itself as shown in methanol-based chain elongation processes;[24,39] therefore it is relevant to reveal whether BES could have an effect on plastic hydrolysates fermentation.

In this study, we developed a tandem strategy for converting PHA and PLA waste into carboxylates through hydrothermal pretreatment followed by open-culture anaerobic fermentation. We evaluated the influence of pretreatment conditions (temperatures, duration, and chemical supplementation) on PHA depolymerization, including synergistic effects from PLA addition and carboxylate supplementation. The process was further validated using commercial products from PHA (drinking cups) and PLA (coffee lids). Subsequently, a continuous stirred tank reactor (CSTR) was operated with sequential feeding of crotonate, PHA hydrolysates, lactate, PLA hydrolysates, and ethanol to evaluate substrate co-fermentation and system stability. 2-Bromoethanesulfonate sodium (BES) was supplied in the medium; except in the last phases to assess whether it affected the fermentation process. The microbial community dynamics were tracked across phases to elucidate bacterial community adaptation and functional enrichment. The integrated process achieved up to ~90% COD conversion from mixed PHA and PLA pellets into carboxylates, demonstrating a potential scalable route for biodegradable plastic valorization. The novel highlights of this study include: (i) the demonstration on enhanced depolymerization by mixing PHA and PLA, (ii) the development of a first continuous fermentation process using plastic hydrolysates as a substrate, and (iii) the presentation of a first microbial community analysis from a carboxylate production bioprocess with hydrolyzed biodegradable plastics as feedstock.

Experimental

Materials

The PHA pellets used in this study were ENMAT™ Thermoplastics PHBV Resin Y1000P (Ningbo, China), consisting of 98.5% poly(3-hydroxybutyrate-*co*-3-hydroxyvalerate) (PHBV), 1% boron nitride, and 0.5% KY1010 (as the antioxidant)[40] (Fig. S3, SI). The PHBV co-polymer was composed of 98% 3-hydroxybutyrate (3-HB) and 2% 3-hydroxyvalerate (3-HV). The PLA pellets were Ingeo™ Biopolymer 4043D (Natureworks, USA). The PHA beakers were produced by Happy Cups™ (Oosterwolde, the Netherlands) and according to the producer containing the same ENMAT™ PHBV Resin Y1000P pellets and green-colour masterbatch.[41] The PLA lids (type CPLA: crystallized polylactic acid) were obtained from Green Box GmbH & Co. KG (Bremen, Germany). The chemicals used in hydrothermal processing included lactic acid (90%, VWR, a variable mixture of D- and L-lactic acids), acetic acid (>99%, Sigma-Aldrich), and crotonic acid (Sigma-Aldrich). Additionally, 3-hydroxybutyric acid (≥98.0%, Sigma-Aldrich), sodium L-lactate (≥99%, Sigma-Aldrich), 2-bromoethanesulfo-

nate sodium (BES, 98%, Alfa), ethanol (96%, VWR), *n*-butyric acid (99%, Sigma-Aldrich), *n*-caproic acid (>99%, Sigma Aldrich), and yeast extract (Merck) were used in the fermentation process. The microbial growth medium composition for open-culture fermentation followed a previously established formulation (Table S1, SI).[14] A 4 mol L^{-1} KOH solution was prepared for pH adjustment before fermentation, and a 1 mol L^{-1} KOH solution was used to control pH during fermentation.

Hydrothermal pretreatment (HTP)

HTP was conducted in a 1 L bench-top stirred reactor (Parr 4857, Parr Instruments Moline, Illinois, USA) (Fig. S1, SI).[42] The reactor was loaded with 700 mL of demineralized water and 35 g of PHA pellets for single PHA hydrolysis under various temperature and reaction time conditions. After loading the feedstocks, the reactor was sealed and operated in batch mode. The process involved a heating phase followed by a controlled cooling procedure, after which the products were analyzed. The heating rate was 4 °C min^{-1} (Fig. S2, SI). The reactor was continuously stirred at 85 rpm using a magnetic agitator throughout the HTP process. At the end of the reaction, the system was rapidly quenched to ~30 °C and returned to atmospheric pressure by opening a cooling loop. Once cooled to room temperature, N_2 gas was flushed through the reactor for 30 seconds to remove potential gaseous byproducts. After N_2 flush, the reactor was opened, and solid and liquid products were collected and filtered using a paper filter (4–7 μm, Schleicher & Schuell 595 1/2). The filtered liquid was stored at 4 °C, while the remaining solids were 48 hours dried in an oven at 50 °C, which is the same temperature advised for PHA storage at minimized moisture uptake.[43] The reactor was cleaned after each experiment using 0.05 M NaOH, heated to 160 °C for 20 minutes, and then cooled to room temperature.

Initial experiments (Table 1, exps. A–F) were conducted at 140 °C–160 °C, with reaction times ranging from 2.5 to 22 hours, to determine conditions under which significant amounts of solid PHA remained. These conditions provided insights into the potential effects of additional supplements on PHA depolymerization. For the HTP of PHA with supplements (exps. G–M), 35 g of PHA pellets (19.6 ± 0 grams carbon) were processed in 700 mL of demineralized water and hydrolyzed for 15 hours at 150 °C, with the addition of 0.1 M carboxylates or bioplastics. To investigate the dissolution efficiency of mixing bioplastic products, 50 g L^{-1} PHA beaker and/or PLA lids (0.1 M) were hydrothermally processed in triplicate (exps. N–P). Additionally, to generate fermentation substrates, 50 g L^{-1} PHA pellets were hydrothermally pretreated at 160 °C for 15 hours (exp. Q), after which the filtered hydrolysates were 10 times diluted and used for fermentation (Table 2, Phases III & IV). Separately, 100 g L^{-1} PHA pellets and 50 g L^{-1} PLA pellets were hydrothermally processed at 150 °C for 15 hours (exp. R), and the resulting hydrolysates were 10 times diluted for microbial conversion (Table 2, Phases V, VI, & VII).

Open-culture fermentation

Following hydrothermal pretreatment, fermentation was conducted in a 3 L continuous stirred tank reactor (CSTR) with a 1.5 L working volume and 1.5 L headspace (Fig. S4, SI). pH, temperature, and gas flow were regulated using the "BearTree" program (Zoetermeer, the Netherlands). The pH was maintained at 5.9 *via* a Watson-Marlow peristaltic pump (Falmouth, Cornwall TR11 4RU, UK), which delivered 1 M KOH as needed. The fermentation temperature was kept at 35 °C using a water bath (Julabo F25, the Netherlands). N_2 (45 mL min^{-1}) and CO_2 (5 mL min^{-1}) were continuously supplied *via* Gas Flow Controllers (Bronkhorst®, the Netherlands), while the effluent gas flow rate was measured using a flow meter (BPC

Table 1 Overview of hydrothermal pretreatment (HTP) of PHA/PLA with additional supplements

No.	Temperature (°C)	Reaction time (h)	Feedstocks	Supplements
A	160	22	PHA pellets (50 g L^{-1})	—
B		15		
C		6		
D		2.5		
E	150	15		
F	140	15		
G	150	15	PHA pellets (50 g L^{-1})	PLA pellets (0.1 M)[a]
H				PHA hydrolysates (0.1 M)[b]
I				Fermentation nutrients (0.1 M)[c]
J				Lactic acid (0.1 M)[d]
K				Crotonic acid (0.1 M)
L				Acetic acid (0.1 M)
M			—	PLA pellets (0.1 M)
N	150	15	PHA beaker (50 g L^{-1})	—
O				PLA lid (0.1 M)
P			—	PLA lid (0.1 M)
Q	160	15	PHA pellets (50 g L^{-1})	—
R	150	15	PHA pellets (100 g L^{-1})	PLA pellets (50 g L^{-1})

Notes: '—' means no addition. [a] The 0.1 M PLA means the amount of fully hydrolyzed PLA would theoretically be equivalent to 0.1 M lactic acid. [b] The PHA hydrolysates (330 mL) used as supplement in '*H*' were obtained from a previous PHA hydrolysis step. [c] Stock solutions, vitamins, and trace metals were added, while yeast extract was omitted. [d] A mixture of D- and L-lactic acid (90%) was used.

Table 2 Experimental setup for the open-culture fermentation of PHA and PLA hydrolysates

Phase	Duration (days)	Substrates	BES addition (5 g L^{-1})
I	0–9	Crotonate (5 g L^{-1})[a] – batch	Yes
II	9–30	Crotonate (5 g L^{-1})[a]	Yes
III	30–54	Crotonate (5 g L^{-1}) + PHA (5 g L^{-1}) hydrolysates[b]	Yes
IV	54–75	Crotonate (5 g L^{-1}) + PHA (5 g L^{-1}) hydrolysates[b] + Na L-lactate (5 g L^{-1})	Yes
V	75–95	PHA (10 g L^{-1}) and PLA (5 g L^{-1}) hydrolysates[c]	Yes
VI	95–113	PHA (10 g L^{-1}) and PLA (5 g L^{-1}) hydrolysates[c]	No
VII	113–132	PHA (10 g L^{-1}) and PLA (5 g L^{-1}) hydrolysates[c] + ethanol (7 g L^{-1})	No

[a] Crotonate was prepared by adding 5 g L^{-1} crotonic acid and adjusting pH by 4 M KOH. [b] 50 g L^{-1} PHA pellets were hydrothermally pretreated at 160 °C for 15 hours (Table 1, exp. Q), and the filtered hydrolysates were 10 times diluted and used for Phases III & IV. [c] 100 g L^{-1} PHA pellets and 50 g L^{-1} PLA pellets were run at 150 °C for 15 hours (Table 1, exp. R), after which the filtered hydrolysates were 10 times diluted and supplied for Phases V, VI, & VII.

Instruments AB, Sweden). The hydraulic retention time (HRT) was set to 3 days (Fig. S7, SI) using a peristaltic pump (Ismatec®, ISM4408, Germany). The inoculum (10 mL) was sourced from rumen liquid (collected from the Animal Science Department, Wageningen University and Research) and effluents from ethanol-, lactate-, and glucose-based fermentation.[44]

The fermentation process was structured into seven phases to investigate the microbial conversion of bioplastic-derived substrates, as outlined in Table 2. The pH of influent medium was adjusted to 5.9 using 4 M KOH, and the bioreactor pH was maintained at 5.9 by 1 M KOH during fermentation. First, batch fermentation was initiated using 5 g L^{-1} crotonate (Phase I), followed by continuous crotonate fermentation at the same concentration (Phase II). In Phase III, 5 g L^{-1} PHA hydrolysates were introduced with the crotonate solution for co-fermentation. Subsequently, 5 g L^{-1} sodium L-lactate was added (Phase IV) to evaluate its effect on fermentation/chain elongation dynamics. A hydrolysate mixture produced through HTP was introduced into the reactor in Phase V, including 10 g L^{-1} PHA and 5 g L^{-1} PLA hydrolysates. The next phase (Phase VI) was identical to Phase V, except that no methane inhibitor (BES) was added, allowing for evaluation of the effect of BES removal on fermentation. Finally, in Phase VII, an additional 7 g L^{-1} ethanol was introduced to examine its impact on co-fermentation under the conditions established in Phase VI.

Sampling and measurement

Following hydrothermal processing, total organic carbon (TOC) in the liquid phase was analyzed using a Shimadzu TOC-5000A analyser. Samples were pre-filtered (0.45 μm) and automatically acidified with H_2SO_4, converting inorganic carbon (carbonates) into CO_2, which was flushed out with CO_2-free synthetic air. The remaining organic carbon was oxidized to CO_2 at 680 °C and detected using a Non-Dispersive Infrared (NDIR) detector. Calibration was performed in the 0–100 mg L^{-1} range.

Soluble COD was measured with LCK 014 kits (HACH GmbH, Germany) after filtration by 0.45 m membrane and an appropriate dilution of the filtrate. The total COD of the PHA (1588 g COD per kg PHBV pellets on average) and PLA (1281 g COD per kg PLA pellets on average) were measured by the COD digestion unit (C. Gerhardt Analytical Systems, Germany) (Table S7, SI).[14]

During fermentation, pH, gas, and liquid samples were collected thrice weekly. Gas-phase components (N_2, O_2, CH_4, and CO_2) were analyzed using a gas chromatograph (Shimadzu GC-2010, Japan) equipped with Porabond Q (50 m × 0.53 mm × 10 μm) and a Molsieve 5A column (25 m × 0.53 mm × 50 μm), using H_2 as the carrier gas (0.6 bar). H_2 was quantified separately using another gas chromatograph (GC, HP-5890, Hewlett Packard, Agilent, USA) equipped with an HP Molsieve 5A column (30 m × 0.53 mm × 25 μm) and argon as the carrier gas.

For liquid sampling, 8 mL of liquid was collected each time. 0.5 mL of this was allocated for pH determination, while the remaining liquid samples were filtered through a 0.45 μm membrane (CHROMAFIL Xtra, Machinerey-Nagel, Germany) and promptly stored at −20 °C for further analysis. Carboxylates and alcohols were quantified using gas chromatography (GC, Agilent 7890B, Agilent, USA) with an HP-FFAP column (25 m × 0.32 mm × 0.50 μm), using nitrogen as the carrier gas. 3-HB, crotonate, and L-lactate were determined *via* high-performance liquid chromatography (HPLC, Thermo Dionex Ultimate 3000 RS), equipped with a UV-RI detector (254 nm) and an Astec CLC-L Chiral column (15 cm × 4.6 mm × 5 μm) along with a prefilter. The column temperature was maintained at 25 °C, and 5 mM $CuSO_4$ was used as the eluent at a continuous flow of 0.15 mL min^{-1}. The injection volume was 50 μL. Chromatography data were analyzed using Chromeleon software (version 7.3). Error bars indicate the standard deviation of triplicate measurements during the HTP experiments, as well as the standard deviation of the average values calculated for each fermentation phase.

Calculations

Identifying the components of solid residues after paper filtration—potentially including oligomers or undetected monomers—was besides visual inspection (see Fig. S5, SI) not fully characterized. To allow mass balance calculations, all undissolved residues and non-quantified hydrolysates were conservatively assumed to be solid PHA residue. For consistency in

estimating polymer input, PHA-based beakers were considered equivalent to commercial PHA pellets, and PLA-based lids were assumed to correspond to PLA pellets, as the presence and composition of any additives were not determined or available. The carbon content of PHA pellets was calculated based on the molecular weight (SI).

During fermentation process, the detailed calculations such as the total dissolved inorganic carbons, volumetric conversion rates, and thermodynamic calculations are provided in the SI.[26,45,46] The error bars in the figures or in text (as ±) represent the standard deviation.

Microbial community analysis

Biomass samples were collected from the fermentation broth at each phase-change point besides Phase II (continuous single crotonate fermentation). The sampling procedure involved homogenizing the fermentation broth by repeatedly drawing and releasing the liquid ten times with a 10 mL syringe, effectively resuspending the immobilized biomass.[47] Around 120 mL broth was sampled at each sampling point and centrifugated at 4000 RPM for 5 minutes, the pellets after discarding the supernatant were rinsed in liquid nitrogen for about 30 seconds, and subsequently stored in a −80 °C freezer until used for microbial community analysis.

The microbial cells were physically lysed, genomic DNA (gDNA) was extracted, and its concentration was verified using a Qubit fluorometer. For each sample, 10 ng of gDNA was transferred to a polymerase chain reaction (PCR) tube and adjusted to 15 μL with nuclease-free water. The 16S Barcoding Kit 24 V14 (SQK-16S114.24) was employed for barcoded PCR amplification using LongAmp Hot Start Taq 2X Master Mix. Amplification conditions included an initial denaturation at 95 °C for 1 min, followed by 25 cycles of 95 °C for 20 s, 55 °C for 30 s, and 65 °C for 2 min, with a final extension at 65 °C for 5 min. Barcoded samples were pooled in equimolar ratios and purified using AMPure XP beads. The pooled library was then ligated with a Rapid Adapter (RA) and quantified before sequencing.

The prepared library was loaded onto an R10.4.1 Flow Cell (FLO-MIN114) after priming with Flow Cell Flush (FCF) mixed with Bovine Serum Albumin (BSA) for improved sequencing performance. Sequencing was conducted using MinKNOW software for data acquisition and basecalling. A species-level taxonomic abundance for full-length 16S reads followed the protocol, with post-sequencing analysis performed using the EPI2ME 16S amplicons and identifying bacterial taxa.[48] Canoco 5 was used to make an Unconstrained Principal Component Analysis (PCA) (Fig. S10, SI) to support discussed correlations.[49]

Results and discussion

Hydrothermal co-processing of PHA/PLA and supplements

The hydrothermal pretreatment (HTP) process was developed to be effective at 150 °C and 15 hours reaction time to depolymerize mixed PHA and PLA plastics. This resulted in a dissolution efficiency of 91 ± 4% corresponding to a conversion of 22.3 g COD per L of total feedstock into 20.5 g COD per L of soluble COD in the hydrolysates (Table S7, SI). The hydrolysate was dominated by 3-hydroxybutyric acid, indicating selective depolymerization of PHA. Notably, the addition of specific chemical supplements, particularly carboxylic acids, further enhanced hydrolysis performance, whereas nutrients from the water supply alone had no significant effect.

The efficiency of PHA hydrolysis increased substantially with higher temperatures and longer reaction times, reaching a maximum yield of 99% at 160 °C for 22 hours (Table S2, SI). In contrast, milder conditions reduced hydrolysis efficiency: 0% dissolution was observed at 160 °C for 2.5 hours, and 7% at 140 °C for 15 hours. Under the moderate condition of 150 °C for 15 hours, 46 ± 8% of PHA dissolved. Solid residues were observed on cooling circuits after HTP (Fig. S5A and B, SI), likely originating from undissolved or re-precipitated mini/microplastics. These observations led to the selection of 150 °C and 15 hours as baseline conditions to assess the catalytic effects of various chemical supplements.

Co-hydrolysis of PHA with PLA significantly enhanced PHA depolymerization by approximately 98% more dissolution, leading to the highest conversion efficiency of 3-hydroxybutyric acid among all tested supplements (Fig. 1, experiments E & G and Table S3, SI). When PHA was hydrolyzed with 0.1 M PLA (exp. G), dissolution increased from 46 ± 8% (PHA alone) to 91 ± 4% (Table S4, SI). The hydrolysates consistently contained 3-hydroxybutyric acid as the major monomer (80–83%) for exp. E & G (Table S5, SI), while crotonic acid remained a minor component (3–4%). Addition of 0.1 M hydrolyzed PHA (exp. H) led to moderate improvement (65 ± 8% dissolution), while fermentation nutrient addition without carboxyl-based supplements (exp. I) had negligible impact (44 ± 3%). These results highlight the potential of PLA co-processing and carboxylic acids (*e.g.*, lactic, crotonic, and acetic acid in exps. J–L) in promoting PHA depolymerization.[30] Meanwhile, single PLA hydrolysis was nearly complete, with 91 ± 1% of the PLA converted into lactic acid.

In all HTP experiments, the pH dropped to around 2.6, and no significant difference on pH were observed among supplements (Table S6, SI). Only when PLA was supplemented, there was slightly lower pH reaching 2.3 ± 0.0. The enhanced catalytic effect observed during PLA co-hydrolysis is likely due to localized acidification and PLA oligomer interactions that accelerate PHA surface depolymerization. While both lactic acid and PLA reduced pH (Table S6, SI), the gradual *in situ* release of acid from PLA may have produced micro-acidic environments around the PHA surface, enhancing erosion and polymer chain cleavage.[50,51] To better understand such potential phenomenon the pH should be measured over time and ideally the local pH of the PHA surface. Additionally, PHA and/or PLA oligomers or residual additives may have acted as catalysts or altered surface properties, further facilitating hydrolysis.[52] These effects may not be replicated by direct addition of monomeric lactic acid. Commercial PLA often contains pro-

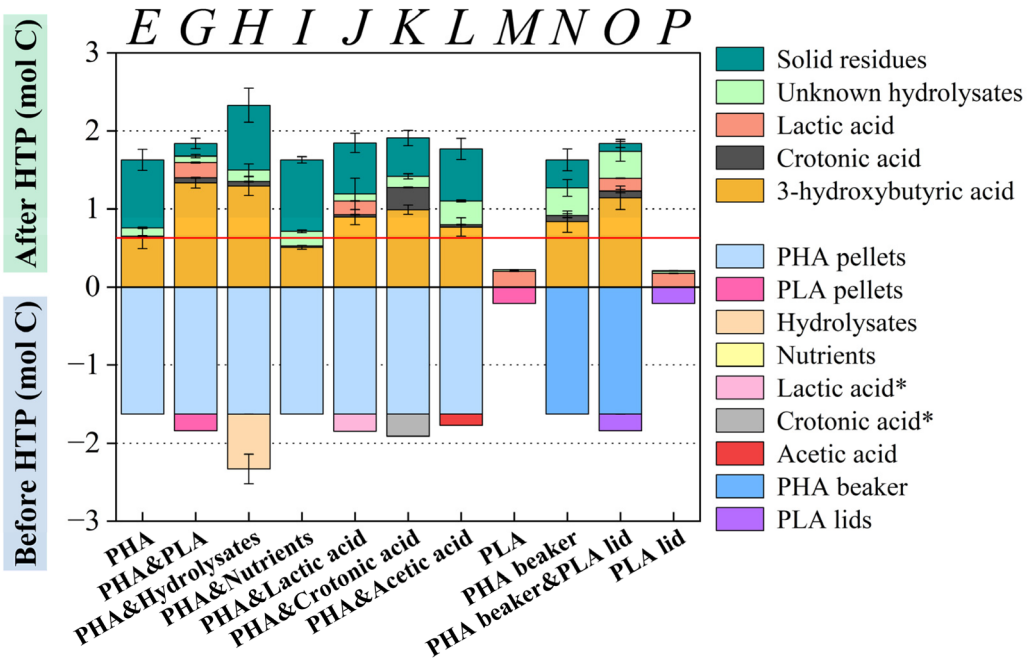

Fig. 1 Effect of various supplements on PHA hydrolysis, expressed as molar carbon (mol C). **E**. HTP of PHA alone (reference). **G**. HTP of PHA with 0.1 M PLA pellets; assumes fully hydrolysis of PLA yields 0.1 M lactic acid. **H**. HTP of PHA with filtered PHA hydrolysates. **I**. HTP of PHA with added inorganic nutrients for fermentation. **J**. HTP of PHA with 0.1 M lactic acid. **K**. HTP of PHA with 0.1 M crotonic acid. **L**. HTP of PHA with 0.1 M acetic acid. **M**. HTP of 0.1 M PLA pellets alone. The red line indicates the 3-hydroxybutyric acid concentration resulting from PHA depolymerization alone (exp. E). 'Lactic acid*' and 'Crotonic acid*' refer to externally added lactic acid and crotonic acids, respectively. The 'Unknown hydrolysates' include oligomers and additives.

prietary co-polymers or additives, such as montmorillonite or plant-based residues,[53,54] which may influence hydrolysis kinetics. In this study, PHBV pellets include 1% boron nitride and 0.5% KY1010,[40] while PLA additives remained unidentified, warranting further chemical characterization of hydrolysates.

The hydrolysates generated in this study exhibited a remarkably high selectivity for 3-hydroxybutyric acid over crotonic acid, with molar ratios up to 28 : 1 (Table S5, SI). This is significantly higher than ratios reported under alkaline (2 : 1 at 70 °C up to 75% decomposition) or milder acidic conditions (4.7–10.3 at 200 °C).[30,55] Carboxylic acid-supplemented HTP further increased these ratios (10–28), whereas neutral conditions using sodium formate or butyrate produced the inverse, favouring crotonic acid (ratios 0.4–0.5).[30] These results suggest that acidic conditions, particularly with co-catalytic compounds, promote selective cleavage mechanisms that favour 3-hydroxybutyric acid production, which is desirable for downstream applications such as microbial fermentation into carboxylates as proposed in present study.

The applicability of HTP technology to commercial bioplastic products was confirmed through the treatment of mixed PHA–PLA items, achieving high dissolution yields without chemical catalysts. A co-mixture of a PHA beaker and PLA lids reached 94 ± 3% dissolution, with 66 ± 8% of the hydrolysates as 3-hydroxybutyric acid (Tables S4 & S5, SI). Single PHA beaker hydrolysis resulted in 51 ± 8% dissolution with similar acid composition (66 ± 7%), while PLA lid achieved 97 ± 1% dissolution, producing predominantly lactic acid (86 ± 1%) along with plausible PLA oligomers. These findings demonstrate that co-hydrolyzing PHA with PLA provides an effective approach to enhancing dissolution without the need for additional chemicals (*e.g.*, alkaline catalysts).[14] However, the faith of (residual) components from colorants or other potential additives remains unknown; evidently visible residues were present (Fig. S5C and D, SI) and suggesting the need for further pretreatment or residue removal steps.

Finally, the catalytic enhancement of PHA hydrolysis by its own hydrolysates or common fermentation intermediates suggests a promising zero-waste route for a more closed-loop bioplastic recycling. The addition of crotonic acid or previously hydrolyzed PHA improved dissolution efficiency, indicating that hydrolysates can function as both substrates and catalysts. This way one can possibly produce catalysts from PHA containing waste streams, and in case not all hydrolysates are used for fermentation, a part of the hydrolysates could retain in the hydrolysis reactor and be used as catalyst to boost the hydrolysis from the start of the hydrothermal process. Wastewaters rich in organic acids, such as fermentation effluents from sludge-derived streams or evenly from the envisioned biodegradable plastic fermentation process, may also be repurposed as catalytic media for HTP, integrating well with wastewater treatment infrastructure.[56] Supply of organic acids (like the tested acetic acid) with hydrolysates compounds do not necessarily hinder the anaerobic fermentation process since

acetate is a fermentation product. However, earlier work on crotonate fermentation showed that adding organic acids (like acetate, propionate or *n*-butyrate) created a lag time on the crotonate fermentation, although it did not prevent the process from proceeding.[26] Moreover, the resulting low pH hydrolysates—rich in carboxylic acids—are not only valuable intermediates for PHA re-synthesis, but it is also suitable as an acid media to do pH control during fermentation which tend to have an increasing pH like lactate-based chain elongation.[57,58]

Open-culture fermentation of PHA and PLA hydrolysates

Batch and continuous crotonate fermentation into acetate and *n*-butyrate (Phases I–II). Acetate and *n*-butyrate were the dominant products during both batch and continuous crotonate fermentation under mildly acidic conditions (Fig. 2D). Nearly complete conversion of 233 mM C crotonate (5 g L^{-1}) resulted in 120 mM C acetate (3.6 g L^{-1}) and 100 mM C *n*-butyrate (2.2 g L^{-1}), with stable acetate-to-*n*-butyrate molar ratios of 2.6 ± 0.3 in Phase I and 2.4 ± 0.1 in Phase II (Fig. 2A, C and Table S8, SI). This product profile is consistent with earlier studies on crotonate fermentation.[26] Carbon recovery was close to 100% (Fig. S6A, SI), and only trace amounts of *n*-caproate, propionate, and i-butyrate were produced (Fig. 2B).

Although previous reports at neutral pH observed negligible CO_2 production,[26] considerable fluctuations (−5 to 14 mmol day^{-1}) were detected at pH 5.9 in this study, even though headspace CO_2 content remained constant at 6.9% (Fig. S6B and C, SI). H_2 levels stayed below 0.03% (Fig. S7B, SI), likely originating from crotonate metabolism[35,59] or minor contributions from yeast extract fermentation.[60]

Co-fermentation of PHA hydrolysate and crotonate (Phase III). Co-fermenting crotonate with PHA hydrolysates preserved the acetate-to-*n*-butyrate ratio observed in crotonate-only fermentations (Fig. 2D). PHA pellets (50 g L^{-1}) were pretreated at 160 °C for 15 hours, and the resulting filtrate was diluted tenfold and subsequently co-fed with 5 g L^{-1} crotonate. During Phase III, 233 mM C crotonate and 180 mM C 3-hydroxybutyrate (3-HB, 4.7 g L^{-1}) were converted into 210 mM C acetate (6.3 g L^{-1}) and 180 mM C *n*-butyrate (4.0 g L^{-1}) (Fig. 2A). The acetate-to-*n*-butyrate ratio remained nearly identical to Phase II (2.4 ± 0.0 *vs.* 2.4 ± 0.1), even though the 3-HB-to-crotonate molar ratio varied (1.0 ± 0.1 *vs.* solely crotonate) (Table S8, SI), suggesting that 3-HB and crotonate may undergo similar metabolic conversions. This observation is supported by earlier work reporting an acetate-to-*n*-butyrate ratio of 2.27 for 3-HB fermentation alone.[61] In addition to the main products, trace amounts of propionate and *n*-valerate formation (Fig. 2B) likely originated from 3-hydroxyvalerate (3-HV), a component of PHBV (2% 3-HV) hydrolysis.[62] The metabolic performance of 3-HV needs further investigation.

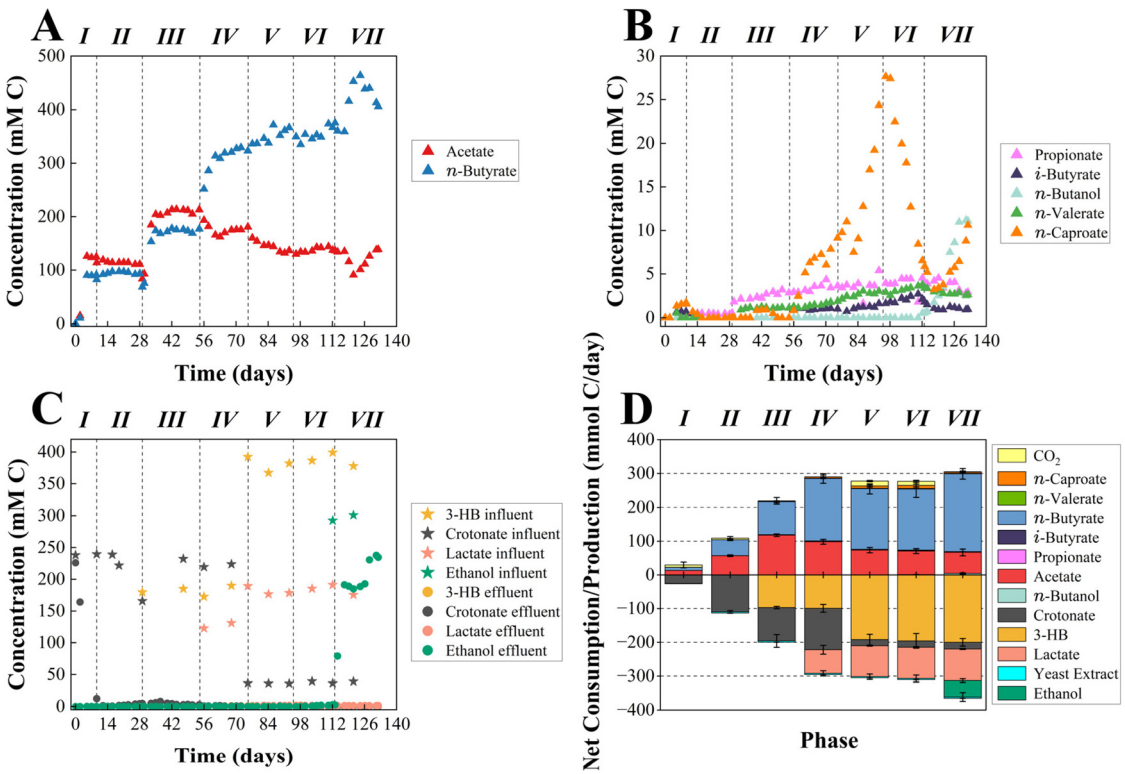

Fig. 2 Carbon fluxes and metabolite dynamics during open-culture fermentation of bioplastic hydrolysates across different phases. (A) Temporal profiles of major carboxylates: acetate and *n*-butyrate (mM C). (B) Concentrations of minor products: propionate, i-butyrate, *n*-valerate, *n*-butanol, and *n*-caproate (mM C). (C) Influent *vs.* effluent concentrations of key substrates: 3-HB (3-hydroxybutyrate), crotonate, lactate, and ethanol (mM C). (D) Net substrate consumption and product production rates (mmol C day^{-1}), based on averaged carbon balances at steady stage.

Lactate co-fermentation enhances *n*-butyrate production and initiates *n*-caproate formation (Phases IV–VI). The addition of lactate markedly increased *n*-butyrate production and triggered *n*-caproate formation. In Phase IV, co-fermenting 130 mM C lactate (~5 g L^{-1} Na L-lactate) with 220 mM C crotonate and 180 mM C 3-HB (from PHA hydrolysates) elevated *n*-butyrate production to 320 mM C (7.0 g L^{-1}), while reducing acetate to 180 mM C (Fig. 2A & C). This shift toward *n*-butyrate resembles previous findings in lactate-driven chain elongation, where *n*-butyrate fermenters outcompeted chain elongators,[63] even though *n*-caproate formation from lactate remains thermodynamically favourable (Fig. S8A, SI).

Notably, the transition from Phase III to IV occurred smoothly without a lag phase, and residual substrate concentrations remained below 3 mM C (<30 mg L^{-1}) (Fig. 2), indicating rapid adaptation to the extra added substrate.

Further fermentation of mixed hydrolysates from PHA (100 g L^{-1}) and PLA (50 g L^{-1}) in Phases V and VI boosted overall product formation. The key change between the phases was BES removal in Phase VI. The combined substrates (~10 g L^{-1} 3-HB and 0.8 g L^{-1} crotonate from PHA; ~5 g L^{-1} L-lactic acid from PLA) produced 360 mM C (7.9 g L^{-1}) *n*-butyrate and 140 mM C (4.2 g L^{-1}) acetate (Fig. 2A & C), with <2 mM C residual substrates. Lactate addition also led to accumulation of i-butyrate (up to 4 mM C in Phase VI), consistent with observations from fermentations using lactate, ethanol, or methanol.[24,49,64]

This process, integrating hydrothermal pretreatment with open-culture fermentation, enabled effective bioplastic conversion. Specifically in Phase VI, 91% of bioplastic COD (22.3 g COD L^{-1}) was solubilized (20.5 g COD L^{-1}) (Table S7, SI). Subsequently, 97% of the SCOD from hydrolysates (mainly 3-HB, crotonate, lactate, and nutrients for fermentation) was converted to carboxylates—72% of which was *n*-butyrate—achieving ~90% overall COD conversion efficiency (Table S7, SI).

H_2 partial pressure ranged from 0 to 0.8 kPa during Phases IV–VI (Fig. S7B, SI). *n*-Caproate increased from trace levels in Phases I–III to 9.1 mM C (176 mg L^{-1}) in Phase IV, peaking at 23.4 mM C (437 mg L^{-1}) in Phase V. This was likely driven by the increased lactate concentration from Phase IV (130 mM C) to V (180 mM C), supporting chain elongation.[25] However, removing BES in Phases VI dropped *n*-caproate to 6.5 mM C (126.6 mg L^{-1}), possibly due to competition from *n*-butyrate fermenters under methanogen-friendly conditions, despite *n*-caproate production is thermodynamically favourable (Fig. S8A and Table S10, SI).[63]

Ethanol addition supports *n*-butyrate and *n*-caproate formation (Phase VII). Ethanol co-feeding further boosted *n*-butyrate production and supported limited *n*-caproate and *n*-butanol formation. Adding 7 g L^{-1} ethanol in Phase VII increased *n*-butyrate to 460 mM C (10.1 g L^{-1}), while acetate decreased to 100 mM C (Fig. 2A). Most 3-HB, crotonate, and lactate were consumed (<2 mM C), but ethanol was only partially utilized (120 mM C) over 13 days (Fig. 2C). *n*-Caproate rose slightly (~10 mM C) (Fig. 2B), consistent with the role of ethanol in supporting chain elongation in both this study and previous work using VFA derived from food waste.[65] These results on the feasibility of continuous co-fermentation of ethanol, and monomers from bioplastics (lactate, 3-HB, and crotonate), align with outcomes previously obtained in batch co-fermentation experiments with selected model compounds.[26]

After day 124, ethanol use and *n*-butyrate formation declined, while acetate levels increased. Possibly *n*-caproate was produced directly from the chain elongation of ethanol and *n*-butyrate.[66] And increased acetate could be derived from ethanol oxidation or acetogenesis (*e.g.*, from CO_2/H_2). Residual ethanol is more often seen during ethanol-based chain elongation processes.[67,68]

n-Butanol was detected, likely formed *via* *n*-butyrate reduction or a potential direct interspecies electron transfer (DIET) rather than the hydroxyl-carboxyl exchange, as *n*-butyrate reduction is thermodynamically favourable (Fig. S8B and Table S10, SI).[24,68] Trace i-butyrate decreased after ethanol introduction, while propionate and *n*-valerate concentrations remained low (Fig. 2B).

Despite BES removal, methane remained undetectable (≪0.01%) (Fig. S7B, SI), potentially due to (1) insufficient adaptation time (Phase VII lasted 19 days *vs.* 15–30 days typically required for methanogen establishment).[69] Still, the used hydraulic retention time (HRT) is three days (Fig. S7C, SI);[70,71] (2) methanogen washout as the bioreactor was only inoculated at the start of fermentation and had been running without re-inoculation for over 100 days; or (3) the inhibitory effect of mildly acidic pH (5.9).[72]

pH self-regulation reduces base consumption. Substrates selection and fermentation pathways strongly influenced KOH demand, with lactate co-fermentation supporting effective pH control. Although fermentation pH was consistently maintained at 5.9 ± 0.1, KOH consumption varied across phases (Fig. S6D, SI). Phase II (crotonate-only) required 237 mmol OH^- per day (using 1 M KOH), which rose to 509 mmol day^{-1} when PHA hydrolysates were included in Phase III. In contrast, adding lactate in Phase IV significantly reduced base demand to 218 mmol OH^- per day. Phases V and VI—featuring PHA & PLA hydrolysates and lactate—required almost no external base, suggesting that lactate-driven metabolism effectively buffered the system by offsetting acid production with proton-consuming reactions.[25]

Nonetheless, external pH adjustment was needed before fermentation started. For instance, pre-adjustment in Phase II required 26.6 mmol OH^- per day of 4 M KOH to reach pH 5.9, contributing to a total base input of 263.6 mmol OH^- per day or 6.5 mol OH^- per mol VFA (Table S9, SI). While pre-adjustment demands were higher in Phases V (73.0 mmol OH^- per day) and VI (84.6 mmol OH^- per day), total base input during PHA & PLA fermentation dropped to 0.9–1.0 mol OH^- per mol VFA—lower than earlier phases, though still slightly above values reported for lactate-based (derived from food waste) chain elongation (0.47–0.77 mol OH^- per mol medium-chain carboxylates).[25] This underscores the importance of pathway

design in reducing chemical inputs and operation costs in carboxylate fermentation processes.

Microbial community analysis

Various microbial species could play a role in metabolizing the provided substrates and producing the various carboxylates and alcohols. Strikingly, *Clostridium tyrobutyricum* emerged as a key species in the reactor microbiome. To investigate the microbial community involved, we employed 16S rRNA long-read sequencing in this study, which provided enhanced taxonomic resolution over conventional short-read approaches.[48] Using this method and the applied bioinformatics pipeline, over 98.9% of the obtained sequence reads could be taxonomically classified using the reference database (Table S11, SI), indicating high classification efficiency. However, this does not fully reflect the native microbial diversity. A dominant expectation-maximization unit (emu), closely affiliated with *Clostridium tyrobutyricum*, rose to exceed 61% relative abundance following crotonate addition (Fig. 3). Although this species is commonly associated with the conversion of cellulose, glucose, and xylose into acetate, *n*-butyrate, CO_2, and *n*-butanol,[73,74] the product spectrum observed in our system (Fig. S10, SI) suggests it may also metabolize crotonate, 3-hydroxybutyrate, and potentially lactate under the conditions tested.

The microbial community shifted significantly from a diverse inoculum to a *Firmicutes*-dominated consortium enriched in *Clostridium* (Fig. 3). The inoculum, derived from a mixture of ethanol-, lactate-, and glucose-based fermentation broths and bovine rumen liquid, was initially dominated by *Pseudomonas caeni* (22%) and *Simplicispira psychrophila* (11%)—both *Proteobacteria*—as well as *Fermentimonas caenicola* (13%) from the phylum *Bacteroidetes*. During fermentation, however, *Firmicutes* became the dominant phylum, comprising more than 90% of the microbial community across all fermentation phases (Fig. S9A, SI). At the genus level, *Clostridium* represented over 78% of the total community (Fig. S9B, SI), reflecting strong selection pressure likely imposed by the nature of the hydrolysates and fermentation conditions.

The introduction of PHA hydrolysates in Phase III led to the enrichment of various species that could possibly present, such as *Ilyobacter delafieldii*, a species with known PHA- and 3-HB-metabolizing capabilities. By the end of Phase IV, which involved co-fermentation of lactate, crotonate, and PHA hydrolysates, a species like *I. delafieldii* reached a relative abundance of 6%. This species is reported to metabolize PHA, 3-HB, and crotonate into acetate and *n*-butyrate,[35] supporting its potential role in the observed product spectrum during these phases.

The removal of the methanogenesis inhibitor (BES) in Phase VI did not notably impact bacterial community composition, although archaeal activity remains to be determined. The structure of the bacterial community in Phase VI was similar to that of Phase V, with a species like *C. tyrobutyricum* maintaining high relative abundance. However, without sequencing data for archaeal populations, it is unclear whether methanogens were flushed out or remained suppressed. Further archaea analysis is required to evaluate the actual impact of BES removal on methanogenic activity.

The addition of ethanol in Phase VII led to notable shifts in microbial composition, characterized by increased relative abundances of species similar to *Clostridium scatologenes* (10%) and *Clostridium luticellarii* (8%). These changes were accompanied by a reduction in *C. tyrobutyricum* abundance from 80% in Phase VI to 61% in Phase VII. *C. luticellarii* and *C. scatologenes* are both capable of converting H_2/CO_2 into

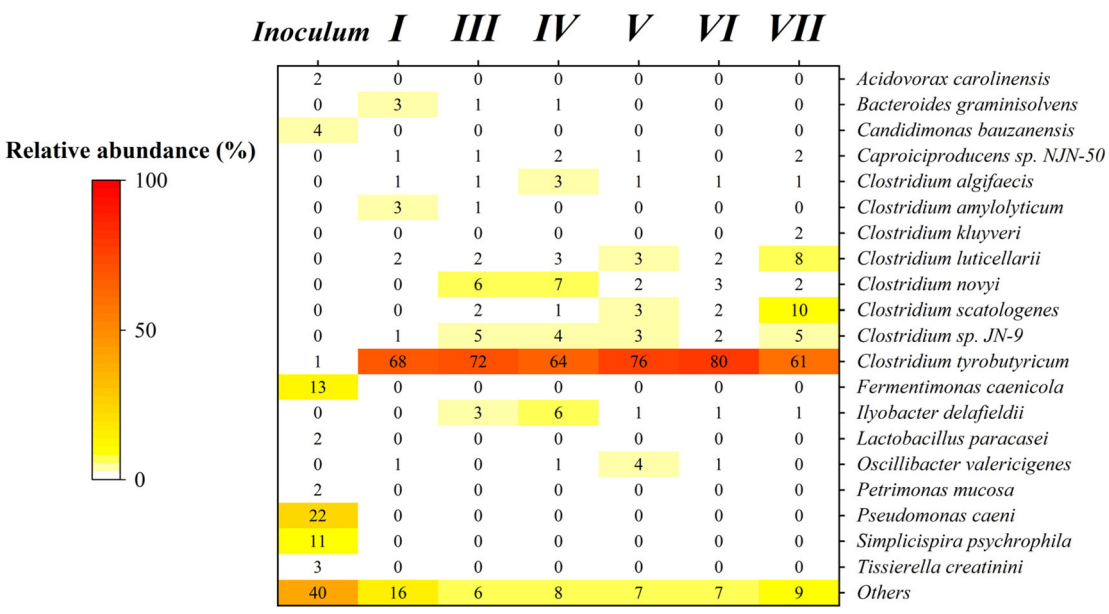

Fig. 3 Heatmap of microbial community composition (species level) by relative abundance determined by 16S rRNA analysis.

acetate and *n*-butyrate.[75,76] Additionally, *C. luticellarii* has been associated with ethanol consumption and i-butyrate production,[45,49] while *C. scatologenes* can utilize CO/H_2 to produce ethanol and *n*-butanol.[76] These findings suggest functional diversification within the *Clostridium* genus in response to ethanol supplementation, enabling expanded substrate use and product formation.

Overall, the microbial community demonstrated notable resilience and adaptability across the different fermentation phases. The introduction of new substrates was consistently accompanied by community shifts, indicating dynamic microbial selection and substrate-driven enrichment. Further in-depth analysis such as isolation and characterization of key strains will be essential to confirm the functional roles of the identified species and to unravel potential interspecies metabolic interactions.[77,78]

Conclusions

This study demonstrates the successful integration of hydrothermal pretreatment and continuous open-culture fermentation for the conversion of PHA and PLA bioplastics into valuable C_2–C_6 carboxylates. Co-hydrolysis of PHA with PLA, or other media like carboxylic acid additions significantly enhanced PHA depolymerization at 150 °C, enabling efficient downstream fermentation. The combination of HTP with fermentation system achieved high COD conversion efficiency (estimated ~90%) and *n*-butyrate selectivity (71%), with acetate and *n*-butyrate as dominant products. Microbial community analysis revealed dynamic shifts in response to substrate changes, with species alike *Clostridium tyrobutyricum* consistently dominating and likely driving the conversion of crotonate, 3-hydroxybutyrate, and lactate into carboxylates. These findings provide new insights into microbial plastic valorization and highlight the potential of open-culture systems for circular bioplastic recycling.

Author contributions

Yong Jin: planned and performed the experiments, analyzed the results and wrote the manuscript. Ralf Beckmans: performed the hydrothermal processing experiments, and data analysis, and reviewed the manuscript. Kasper de Leeuw: data analysis and review of the manuscript. David Strik: concept design, data analysis, and manuscript review.

Conflicts of interest

DS is an employee of Wageningen University & Research (WUR) fulfilling the role of one of the platform managers of Unlock (https://m-unlock.nl/). K. L. works as a lecturer at WUR as well as a senior researcher at ChainCraft (https://chaincraft.com/). The authors declare no conflict of interest.

Data availability

The original data presented in this paper have been placed in the 4TU. Research and are available at following site: https://url.uk.m.mimecastprotect.com/s/pBYcCWL9qSDmgpgh6fruoXhFj?domain=data.4tu.nl. The microbiota raw sequencing data have been deposited in the European Nucleotide Archive (ENA) at EMBL-EBI under accession number PRJEB98625 and are available at following site: https://url.uk.m.mimecastprotect.com/s/jyhkCXL95SOoy6yuVh0uWLgIq?domain=ebi.ac.uk.

Supplementary information (SI) is available. See DOI: https://doi.org/10.1039/d5gc02732b.

Acknowledgements

In this work, we want to express our appreciation to Lucian Wester and Beatriz Alvarado Perry (Wageningen University & Research, Environmental Technology, the Netherlands) for their support in the methods development of 3-hydroxybutyrate and crotonate detection. Also acknowledge the staff of UNLOCK (www.m-unlock.com) for their support on microbial community analysis and dataset treatment. This research was funded by the China Scholarship Council, grant number CSC 202006460010.

References

1 A. Z. Naser, I. Deiab and B. M. Darras, *RSC Adv.*, 2021, **11**, 17151–17196.
2 K. W. Meereboer, M. Misra and A. K. Mohanty, *Green Chem.*, 2020, **22**, 5519–5558.
3 D. P. B. T. B. Strik and B. Heusschen, *Microorganisms*, 2023, **11**, 2103.
4 European Bioplastics, Bioplastics market development update 2024, https://www.european-bioplastics.org/market/#, (accessed 06, February, 2025).
5 D. Merino, A. Zych and A. Athanassiou, *ACS Appl. Mater. Interfaces*, 2022, **14**, 46920–46931.
6 M. van den Oever, K. Molenveld, M. van der Zee and H. t. Bos, *Bio-based and biodegradable plastics: facts and figures: focus on food packaging in the Netherlands*, 2017.
7 TotalEnergies Corbion, Bioplastic value chain partnership delivers new sustainable textiles, https://www.totalenergies-corbion.com/news/bioplastic-value-chain-partnership-delivers-new-sustainable-textiles/, (accessed 13/02, 2024).
8 R. Plavec, S. Hlaváčiková, L. Omaníková, J. Feranc, Z. Vanovčanová, K. Tomanová, J. Bočkaj, J. Kruželák, E. Medlenová, I. Gálisová, L. Danišová, R. Přikryl, S. Figalla, V. Melčová and P. Alexy, *Polym. Test.*, 2020, **92**, 106880.
9 L. Filiciotto and G. Rothenberg, *ChemSusChem*, 2021, **14**, 56–72.
10 S. V. Afshar, A. Boldrin, T. F. Astrup, A. E. Daugaard and N. B. Hartmann, *J. Cleaner Prod.*, 2024, **434**, 140000.

11 A. Abraham, H. Park, O. Choi and B.-I. Sang, *Bioresour. Technol.*, 2021, **322**, 124537.
12 T. D. Moshood, G. Nawanir, F. Mahmud, F. Mohamad, M. H. Ahmad and A. AbdulGhani, *Curr. Res. Green Sustainable Chem.*, 2022, **5**, 100273.
13 Z. Piao, A. A. Agyei Boakye and Y. Yao, *Nat. Chem. Eng.*, 2024, **1**, 661–669.
14 Y. Jin, K. D. de Leeuw and D. P. B. T. B. Strik, *Materials*, 2023, **16**, 2693.
15 W. Zeng, K. D. de Leeuw and D. P. B. T. B. Strik, *ACS Sustainable Chem. Eng.*, 2025, **13**, 8116–8127.
16 L. T. Angenent, H. Richter, W. Buckel, C. M. Spirito, K. J. J. Steinbusch, C. M. Plugge, D. P. B. T. B. Strik, T. I. M. Grootscholten, C. J. N. Buisman and H. V. M. Hamelers, *Environ. Sci. Technol.*, 2016, **50**, 2796–2810.
17 Y. Jin, Y. Lin, P. Wang, R. Jin, M. Gao, Q. Wang, T.-C. Chang and H. Ma, *Bioresour. Technol.*, 2019, **292**, 121957.
18 M. Perez-Zabaleta, M. Atasoy, K. Khatami, E. Eriksson and Z. Cetecioglu, *Bioresour. Technol.*, 2021, **323**, 124604.
19 ChainCraft, In the whole food value chain-from primary agricultural production to the food on your plate-food residues are created, https://chaincraft.com/technology/, (accessed 0205, 2025).
20 AFYREN, Biobased organic acids, https://afyren.com/en/, (accessed 04/04, 2025).
21 BIOVERITAS, BioVeritas can unleash unlimited growth by unlocking more feedstocks and using less energy to deliver the most cost-effective sustainable aviation fuel, https://www.bioveritas.com/, (accessed 04/04, 2025).
22 Capro-X, A circular approach to chemical manufacturing & waste disposal, https://www.capro-x.com/, (accessed 04/04, 2025).
23 M. T. Holtzapple, H. Wu, P. J. Weimer, R. Dalke, C. B. Granda, J. Mai and M. Urgun-Demirtas, *Bioresour. Technol.*, 2022, **344**, 126253.
24 K. D. de Leeuw, T. Ahrens, C. J. N. Buisman and D. P. B. T. B. Strik, *Front. Bioeng. Biotechnol.*, 2021, **9**, 1–14.
25 C. A. Contreras-Davila, V. J. Carrion, V. R. Vonk, C. N. J. Buisman and D. Strik, *Water Res.*, 2020, **169**, 115215.
26 Y. Jin, K. D. de Leeuw and D. P. B. T. B. Strik, *Chem. Eng. J.*, 2025, **517**, 1–10.
27 O. García-Depraect, R. Lebrero, S. Rodriguez-Vega, R. A. Börner, T. Börner and R. Muñoz, *Bioresour. Technol.*, 2022, **360**, 127655.
28 N. Mat Yasin, S. Akkermans and J. F. M. Van Impe, *Waste Manage.*, 2022, **150**, 1–12.
29 M. W. Myburgh, W. H. van Zyl, M. Modesti, M. Viljoen-Bloom and L. Favaro, *Bioresour. Technol.*, 2023, **390**, 129908.
30 Y. Li and T. J. Strathmann, *Green Chem.*, 2019, **21**, 5586–5597.
31 M. Polidar, E. Metzsch-Zilligen and R. Pfaendner, *Polymers*, 2022, **14**, 4237.
32 A. Dhaini, V. Hardouin-Duparc, A. Alaaeddine, J.-F. Carpentier and S. M. Guillaume, *Prog. Polym. Sci.*, 2024, **149**, 101781.
33 M. Stieb and B. Schink, *Arch. Microbiol.*, 1984, **140**, 139–146.
34 P. S. Beaty and M. J. McInerney, *Arch. Microbiol.*, 1987, **147**, 389–393.
35 P. H. Janssen and C. G. Harfoot, *Arch. Microbiol.*, 1990, **154**, 253–259.
36 R. K. Thauer, K. Jungermann, H. Henninger, J. Wenning and K. Decker, *Eur. J. Biochem.*, 1968, **4**, 173–180.
37 W. Logroño, M. Nikolausz, H. Harms and S. Kleinsteuber, *Microorganisms*, 2022, **10**, 1–15.
38 L. Laguillaumie, M. Peyre-Lavigne, A. Grimalt-Alemany, H. N. Gavala, I. V. Skiadas, E. Paul and C. Dumas, *J. Cleaner Prod.*, 2023, **414**, 137549.
39 S. Huang, R. Kleerebezem, K. Rabaey and R. Ganigué, *Appl. Microbiol. Biotechnol.*, 2020, **104**, 5119–5131.
40 Tianan Biologic Material Co., Material Safety Data Sheet ENMAT Y1000, http://en.tianan-enmat.com/pdf/MSDS-Y1000P.pdf, (accessed 28/04/2025, 2025).
41 HappyCups, Happy Cups Bioplastic Drinkbeker PHA Biologisch afbreekbaar 200 mL, https://www.circulaireweb-shop.nl/bioplastic-drinkbeker-pha-biologisch-afb-143232890.html, (accessed 28/04/2025, 2025).
42 T. M. B. Mouthier, Biological and chemical pretreatment of grasses to overcome lignin's recalcitrance improvingcarbohydrate degradability, PhD Thesis, Wageningen University, 2018, DOI: 10.18174/453742.
43 Tianan Biologic Material Co., Technical Data Sheet & Processing Guide ENMAT Y100P, http://en.tianan-enmat.com/pdf/TDS_Y1000P-2024.pdf (accessed 28/04/2025, 2025).
44 C. A. Contreras-Dávila, A. Ali, C. J. N. Buisman and D. P. B. T. B. Strik, *Fermentation*, 2021, **7**, 41.
45 K. D. de Leeuw, M. J. W. van Willigen, T. Vrauwdeunt and D. P. P. T. B. Strik, *Front. Bioeng. Biotechnol.*, 2024, **12**, 1–11.
46 P. Candry, L. Radic, J. Favere, J. M. Carvajal-Arroyo, K. Rabaey and R. Ganigue, *Water Res.*, 2020, **186**, 116396.
47 K. Gemeinhardt, B. S. Jeon, J. N. Ntihuga, H. Wang, C. Schlaiß, T. N. Lucas, I. Bessarab, N. Nalpas, N. Zhou, J. Usack, D. H. Huson, R. Williams, B. Macek, L. Aristilde and L. T. Angenent, *Green Chem.*, 2024, **27**, 2931–2949.
48 K. D. Curry, Q. Wang, M. G. Nute, A. Tyshaieva, E. Reeves, S. Soriano, Q. Wu, E. Graeber, P. Finzer, W. Mendling, T. Savidge, S. Villapol, A. Dilthey and T. J. Treangen, *Nat. Methods*, 2022, **19**, 845–853.
49 K. D. de Leeuw, S. M. de Smit, S. van Oossanen, M. J. Moerland, C. J. N. Buisman and D. P. B. T. B. Strik, *ACS Sustainable Chem. Eng.*, 2020, **8**, 8184–8194.
50 R. Langer and N. Peppas, *J. Macromol. Sci., Part C: Polym. Rev.*, 1983, **23**, 61–126.
51 J. Siepmann and A. Göpferich, *Adv. Drug Delivery Rev.*, 2001, **48**, 229–247.

52 G. Gorrasi and R. Pantani, in *Synthesis, Structure and Properties of Poly(lactic acid)*, ed. M. L. Di Lorenzo and R. Androsch, Springer International Publishing, Cham, 2018, pp. 119–151, DOI: 10.1007/12_2016_12.
53 M. A. Paul, C. Delcourt, M. Alexandre, P. Degée, F. Monteverde and P. Dubois, *Polym. Degrad. Stab.*, 2005, **87**, 535–542.
54 R. Scaffaro, A. Maio and E. F. Gulino, *Compos. Sci. Technol.*, 2021, **213**, 108930.
55 J. Yu, D. Plackett and L. X. L. Chen, *Polym. Degrad. Stab.*, 2005, **89**, 289–299.
56 Torwash, Create 100% recycling of plastics together, https://www.torwash.com/en/plastics/, (accessed 24/03/2025, 2025).
57 J. Myung, N. I. Strong, W. M. Galega, E. R. Sundstrom, J. C. A. Flanagan, S.-G. Woo, R. M. Waymouth and C. S. Criddle, *Bioresour. Technol.*, 2014, **170**, 167–174.
58 C. Samorì, G. A. Martinez, L. Bertin, G. Pagliano, A. Parodi, C. Torri and P. Galletti, *Resour., Conserv. Recycl.*, 2022, **178**, 106082.
59 W. Buckel and R. K. Thauer, *Front. Microbiol.*, 2018, **9**, 1–24.
60 L. Zhang, Q. Ban, J. Li and Y. Xu, *Int. J. Agric. Biol.*, 2014, **16**, 1189–1193.
61 P. H. Janssen and B. Schink, *Biodegradation*, 1993, **4**, 179–185.
62 A. Reischwitz, E. Stoppok and K. Buchholz, *Biodegradation*, 1997, **8**, 313–319.
63 B. Liu, S. Kleinsteuber, F. Centler, H. Harms and H. Sträuber, *Front. Microbiol.*, 2020, **11**, 1–13.
64 B. Liu, D. Popp, N. Müller, H. Sträuber, H. Harms and S. Kleinsteuber, *Microorganisms*, 2020, **8**, 1970.
65 M. Roghair, Y. Liu, D. P. B. T. B. Strik, R. A. Weusthuis, M. E. Bruins and C. J. N. Buisman, *Front. bioeng. biotechnol.*, 2018, **6**, 1–11.
66 S. Bao, Q. Wang, P. Zhang, Q. Zhang, Y. Wu, F. Li, X. Tao, S. Wang, M. Nabi and Y. Zhou, *Energies*, 2019, **12**, 3720.
67 M. Roghair, T. Hoogstad, S. Dpbtb, C. M. Plugge, P. Timmers, R. A. Weusthuis, M. E. Bruins and B. Cjn, *Environ. Sci. Technol.*, 2018, **52**, 1496–1505.
68 K. D. de Leeuw, C. J. N. Buisman and D. P. B. T. B. Strik, *Environ. Sci. Technol.*, 2019, **53**, 7704–7713.
69 I.-S. Lee, P. Parameswaran and B. E. Rittmann, *Bioresour. Technol.*, 2011, **102**, 10266–10272.
70 M. A. Dareioti and M. Kornaros, *Bioresour. Technol.*, 2014, **167**, 407–415.
71 O. Pakarinen, P. Kaparaju and J. Rintala, *Bioresour. Technol.*, 2011, **102**, 8952–8957.
72 S. Qiu, X. Zhang, W. Xia, Z. Li, L. Wang, Z. Chen and S. Ge, *Sci. Total Environ.*, 2023, **877**, 162702.
73 D. Michel-Savin, R. Marchal and J. P. Vandecasteele, *Appl. Microbiol. Biotechnol.*, 1990, **32**, 387–392.
74 J. Lee, Y. S. Jang, M. J. Han, J. Y. Kim and S. Y. Lee, *mBio*, 2016, **7**, 1–12.
75 Q. Mariën, X. Flores-Alsina, U. Aslam, K. V. Gernaey, A. Regueira and R. Ganigué, *Chem. Eng. J.*, 2024, **495**, 153216.
76 Z. Zhu, T. Guo, H. Zheng, T. Song, P. Ouyang and J. Xie, *J. Biotechnol.*, 2015, **212**, 19–20.
77 R. Kleerebezem, G. Stouten, J. Koehorst, A. Langenhoff, P. Schaap and H. Smidt, *Curr. Opin. Biotechnol.*, 2021, **67**, 158–165.
78 W. T. Scott, S. Rockx, Q. Mariën, A. Regueira, P. Candry, R. Ganigué, J. J. Koehorst and P. J. Schaap, *Comput. Struct. Biotechnol. J.*, 2025, **27**, 649–660.

